Journal of Hydroscience and Hydraulic Engineering
Vol. 18, No.2 November, 2000, 75-91

# EDDY CONVECTION VELOCITY AND TAYLOR'S HYPOTHESIS OF 'FROZEN' TURBULENCE IN A ROUGH-BED OPEN-CHANNEL FLOW

By Vladimir Nikora and Derek Goring

National Institute of Water and Atmospheric Research, Christchurch, New Zealand

## SYNOPSIS

An experimental test of Taylor's hypothesis of 'frozen' turbulence, which is implicitly widely used in open-channel hydraulics, is presented. The test is based on two-point velocity measurements with acoustic Doppler velocimeters (known as ADV) in a gravel-bed flow, using methods of cross-correlation functions and time-shift spectra. It is shown that for the flow region $z/H > 0.1$ the eddy convection velocity is close to the local mean velocity and the Taylor hypothesis of 'frozen' turbulence is applicable for mean quantities. For the near-bed flow region, $z/H < 0.1$, the eddy convection velocity demonstrates dependence on eddy scale with the existence of three scale regions with different types of dispersion relations. These relations can be used for converting time/frequency turbulence characteristics into spatial/wave-number characteristics for the near-bed region. The attached-eddy hypothesis is used to explain anomalous behaviour of the dispersion relation for the near-bed flow region.

## INTRODUCTION

Hydraulic engineers, particularly those concerned with turbulence in open-channel flows, often use Taylor's hypothesis of 'frozen' turbulence either implicitly or explicitly and seldom question its validity. In this paper we address the issue of its validity depending on the location in the water column using measurements from a rough-bed open-channel flow.

In 1938 G. I. Taylor (30) attempted to test his relationship between velocity auto-correlation function and power spectrum. For his analysis he had a velocity frequency spectrum measured at a fixed point in grid-generated turbulence in a wind tunnel, and a spatial auto-correlation function $R(\Delta x)$ measured at several spatial lags $\Delta x$. Thus, the data he had were measured in different domains, temporal and spatial. To convert $R(\Delta x)$ into the time domain Taylor (30) suggested that the temporal change in velocity measured at a fixed point in the flow is identical to spatial change along the line which crosses this point and is oriented along the mean flow. Taylor (30) hypothesised that longitudinal eddy transfer at a fixed point occurs with the local mean velocity without appreciable deformation of eddy structure and, therefore, this suggestion is known as the 'frozen' turbulence hypothesis. Analytically, this hypothesis is equivalent to $R^*(\tau) = R(\Delta x = U_E \tau)$, where $U_E$ is the eddy convection velocity which is assumed to be equal to the local mean velocity $\overline{u}$, and $\tau$ is the time lag. The agreement between $R^*(\tau) = R(\Delta x = \overline{u}\tau)$ and the inverse Fourier transform of the frequency spectrum in Taylor's test appeared to be very good (Taylor (30)). Two achievements made Taylor's (30) paper famous: (*1*) a new hypothesis related statistical properties of turbulence in the spatial (wave-number) domain to those in the time (frequency) domain and *vice-versa*; and (*2*) the first experimental test of this hypothesis. Ironically, the initial aim of the paper to test the relationship between the correlation function and the spectrum using experimental data appeared not to be important since that relationship had been rigorously justified earlier by Khinchin (11) (thus, the relationship does not require experimental validation).

Very soon after Taylor's (30) paper appeared it became extremely popular among experimentalists, since it gave a method for converting measurements at fixed points into the spatial domain. Such a conversion is necessary if one is interested in getting information about the spatial structure of turbulence, as well as to test theoretical developments, as most of them are formulated in terms of spatial structure. The importance of this problem for turbulence research and engineering has initiated a number of studies which have mainly been conducted in the atmospheric boundary layer, wind tunnels, and pipes (Monin and Yaglom (15), Piomelli et al. (27)). There have been some inconsistencies even for these well studied conditions and the question of the validity of Taylor's hypothesis remains (Zaman and Hussain (33); Perry and Li (25); Kaimal and Finnigan (10); Pinton and Labbe (26)). However, many researchers implicitly regard this hypothesis as fully validated and use it extensively in their experimental work. The applicability of the 'frozen' turbulence hypothesis for river flows, which in some respects are different from the atmospheric boundary layer and pipes (Monin and Yaglom (15); Nezu and Nakagawa (16)), was examined in Grinvald and Nikora (6), Nikora and Ekhnich (18), Nikora (17), and Shteinman et al. (29). These studies were restricted to fixed beds and the longitudinal velocity component only.

In this paper we extend the previous analyses for river flows, mentioned above, for the case of weakly-mobile beds. Also, in contrast to these studies, we analyse all three velocity vector components as well as a passive substance, and consider potential dependence of the eddy transfer velocity on eddy scale. A theoretical background is presented first, then we outline the methods and experiments used in our analysis, present the results, compare them with previous studies, discuss their potential applications in hydraulic engineering, and, finally, summarise our conclusions.

## THEORETICAL BACKGROUND

In analytical form, Taylor's hypothesis states that:

$$\frac{\partial \phi}{\partial t} = -U_E \frac{\partial \phi}{\partial x} \quad \text{or} \quad \overline{(\frac{\partial \phi}{\partial t})^2} = U_E^2 \overline{(\frac{\partial \phi}{\partial x})^2} \tag{1}$$

$$R(\tau) = R(\Delta x = U_E \tau) \tag{2}$$

$$D(\tau) = D(\Delta x = U_E \tau) \tag{3}$$

$$U_E S_p(\omega) = S_p(k_w = \omega / U_E); \qquad k_w = \frac{1}{U_E}\omega \tag{4}$$

where $U_E = \overline{u}$, $\phi$ = flow quantity of interest (velocity components or passive substance $S$); $R(\tau)$ and $D(\tau)$, $R(\Delta x)$ and $D(\Delta x)$ = temporal and spatial correlation and structure functions, respectively; $S_p(\omega)$ and $S_p(k_w)$ = frequency ($\omega$) and wave-number ($k_w$) spectra, respectively. Relationships (1) to (4) may be valid only approximately and only for some special flow conditions. For the case of homogeneous turbulence with constant (in space) mean velocity $U_o$, it can be readily shown (Monin and Yaglom (15)), using the Navier-Stokes equations, that the mean square of the relative error $\overline{\varepsilon^2}$ of Taylor's hypothesis in the form of (1) for velocity components can be expressed as:

$$\overline{\varepsilon_{ui}^2} = \frac{\overline{(\frac{\partial u_i}{\partial t} + U_o \frac{\partial u_i}{\partial x})^2}}{U_o^2 \overline{(\frac{\partial u_i}{\partial x})^2}} < \alpha_i (\frac{\sigma_{ui}}{U_o})^2 \tag{5}$$

where $u_i$ = velocity vector component (longitudinal $u_1 \equiv u$, transverse $u_2 \equiv v$, or vertical $u_3 \equiv w$); $x$, $y$, and $z$ are the longitudinal, transverse and vertical coordinates, respectively; $\sigma_{ui} = (\overline{u_i'^2})^{0.5}$ = standard deviation of the *i-th* velocity component, where $u_i'$ = velocity deviation from the mean value $\overline{u}_i$, $u_i' = u_i - \overline{u}_i$; an overbar defines the operation of time averaging; and $\alpha_i$ = some constants of the order of 10 (Monin and Yaglom (15)). An analogous relationship may be derived, following a similar procedure as in Monin and Yaglom (15) and using the advection-diffusion equation, for a passive substance $S$:

$$\overline{\varepsilon_s^2} = \frac{\overline{(\frac{\partial S}{\partial t} + U_o \frac{\partial S}{\partial x})^2}}{U_o^2 \overline{(\frac{\partial S}{\partial x})^2}} < \beta (\frac{K^{0.5}}{U_o})^2 \qquad (6)$$

where $K = 0.5(\overline{u'^2} + \overline{v'^2} + \overline{w'^2})$ = total turbulence energy; and $\beta$ = a constant. We have neglected effects of viscous diffusion and assumed that $\overline{(\partial S/\partial x)^2} \sim \overline{(\partial S/\partial y)^2} \sim \overline{(\partial S/\partial z)^2}$ when deriving (6). The same order is expected for $\beta$ as for $\alpha_i$ in (5). From relationships (5) and (6) it follows that for homogeneous flows the Taylor hypothesis with $U_E = U_o$ should be fairly valid if $\sigma_{ui} << U_o$ or, in more general form, $K^{0.5} << U_o$. Indeed, experiments in quasi-homogeneous flows with low levels of turbulence ($\sigma_{ui}/U_o$ was less than 0.15-0.20) showed good agreement between direct spatial measurements of velocity components and estimations from (1) to (4) (see Monin and Yaglom (15) for a review of the atmospheric and laboratory data).

However, when the level of turbulence is high in homogeneous flows the Taylor hypothesis requires a revision. As an example, from theoretical analyses of Ogura (22) and Gifford (4) it follows that scaling in the frequency (time) domain is different from that in the wave-number (space) domain, if $\sigma_{ui} \geq U_o$. They found that for this special case the structure function $D(\tau) \propto \tau^{\gamma}$ has an exponent $\gamma \approx 1 > 2/3$ when $D(\Delta x) \propto \Delta x^{2/3}$. Some atmospheric measurements (e.g., Hutchings (8)) suggest that with a decrease in $\sigma_{ui}/U_o$ the exponent $\gamma$ tends from 1.0 to Kolmogorov's 2/3 for the inertial subrange. We will discuss these results in relation to ours in *Discussion*. Another example was presented by Pinton and Labbe (1995) who studied the applicability of Taylor's hypothesis for swirling flows and found that for their case study $\gamma$ was less than 2/3 (not larger as in Ogura (22) and Gifford (4) analyses and in Hutchings (8) observations). Both examples suggest that the eddy convection velocity $U_E$ may potentially depend on eddy scale if $\sigma_{ui} \geq U_o$.

For turbulent shear (non-homogeneous) flows like open-channel flows the situation is more complex since measurements at a fixed point may contain eddies which come to the measuring point from flow regions with different mean velocities (due to velocity shear). This implies that the eddy convection velocity may be not constant and may also depend on scale. The latter may be due to various potential scenarios (e.g., small eddies may be transported by large ones, or, alternatively, small and large eddies may travel independently, but with different speed). As a result of these effects criteria (5) and (6) should be supplemented by additional criteria. Relations (1) to (4) will be (approximately) valid for shear flows if the effects of the transverse and vertical velocity shear are not strong, i.e., the following inequalities are satisfied:

$$u\frac{\partial u}{\partial x} >> v\frac{\partial u}{\partial y} + w\frac{\partial u}{\partial z} \qquad (7)$$

$$u\frac{\partial S}{\partial x} >> v\frac{\partial S}{\partial y} + w\frac{\partial S}{\partial z} \qquad (8)$$

Applying Reynolds decomposition for instantaneous flow variables (i.e., $\phi = \overline{\phi} + \phi'$) in (7) and (8), and reasonably assuming for open-channel flows that far from the bed and banks the following relations are acceptable: (1) $\partial u'/\partial z \sim \partial u'/\partial x >> \partial u'/\partial y$; (2) $\partial \overline{u}/\partial z >> \partial \overline{u}/\partial y \sim \partial \overline{u}/\partial x$; (3) $\partial S'/\partial z \sim \partial S'/\partial x >> \partial S'/\partial y$; (4) $\partial \overline{S}/\partial z >> \partial \overline{S}/\partial y \sim \partial \overline{S}/\partial x$; (5) $\overline{v} \approx \overline{w} \approx 0$, and (6) $u' \sim v' \sim w' >> w_o$ ($w_o$ is the settling velocity for suspended sediment if it is considered as a passive substance), we can derive from (7) and (8):

$$\frac{\overline{u}}{u'}\frac{\partial u'}{\partial x} >> \frac{\partial \overline{u}}{\partial z} \tag{9}$$

$$\frac{\overline{u}}{u'}\frac{\partial S'}{\partial x} >> \frac{\partial \overline{S}}{\partial z} \tag{10}$$

To make relationships (9) and (10) more readable we represent the velocity and substance derivatives in terms of appropriate velocity and substance concentration scales, as well as their length scales, i.e., $\partial u'/\partial x \sim \sigma_u/\lambda_u$, $\partial \overline{u}/\partial z \sim U_{max}/H$, $\partial S'/\partial x \sim \sigma_S/\lambda_S$, $\partial \overline{S}/\partial z \sim S_{\max}/H$, where $U_{\max}$ is the maximum mean velocity (e.g., surface velocity), $\sigma_S$ is the standard deviation of substance concentration fluctuations, $\lambda_u$ and $\lambda_S$ are characteristic scales of velocity and substance fluctuations, $S_{\max}$ is the maximum substance concentration, and $H$ is the flow depth. Using these scales we can rewrite (9) and (10) as:

$$\lambda_u << \lambda_{cr} = \frac{\sigma_u}{U_{max}}\frac{\overline{u}}{\sigma_u}H \quad \text{or} \quad k_{wu} >> k_{cr} = 2\pi\frac{U_{max}}{\sigma_u}\frac{\sigma_u}{\overline{u}}\frac{1}{H} \tag{11}$$

$$\lambda_S << \lambda_{crS} = \frac{\sigma_S}{S_{max}}\frac{\overline{u}}{\sigma_u}H \quad \text{or} \quad k_{wS} >> k_{crS} = 2\pi\frac{S_{max}}{\sigma_S}\frac{\sigma_u}{\overline{u}}\frac{1}{H} \tag{12}$$

where $k_{cr} = 2\pi/\lambda_{cr}$ and $k_{crS} = 2\pi/\lambda_{crS}$ = critical wave numbers for velocity and substance, respectively. Relationships (11) and (12) establish approximate upper limits for scales $\lambda_u$ and $\lambda_S$, and lower limits for wave-numbers $k_{wu}$ and $k_{wS}$, which should satisfy Taylor's hypothesis fairly well. Condition (11) should be also applicable for the transverse and vertical velocities. It is worth noting that for both velocities and substance these scale limits are of the same order of magnitude and comparable with the flow depth.

An additional conclusion may be extracted from (9) if we assume that the logarithmic law $\overline{u} = (u_*/\kappa)\ln(z/z_o)$ is approximately valid for most of the flow depth (Grinvald and Nikora (6); Nikora (17)) and so $\partial \overline{u}/\partial z$ can be represented as:

$$\frac{\partial \overline{u}}{\partial z} = \frac{u_*}{\kappa z} \tag{13}$$

With (13) relationships (9) and (11) transform to:

$$\lambda_u << \frac{\overline{u}}{u_*}\kappa z = z\ln(\frac{z}{z_o}) \quad \text{or} \quad k_{wu} >> 2\pi\{z\ln(\frac{z}{z_o})\}^{-1} \tag{14}$$

where $u_*$ = shear velocity; $z_o$ = hydrodynamic roughness length; and $\kappa$ = von Karman constant. Relationship (14) shows that the range of eddy scales, which satisfy Taylor's hypothesis, increases with the distance from the bed, and also depends on the bed roughness. The size of the largest eddy that still can be viewed as 'frozen' decreases logarithmically with increase in bed roughness $z_o$. This means that the biggest eddies which still propagate with convection velocity $\overline{u}$ will be larger in lowland rivers than those in gravel-bed rivers.

The condition (14), which accounts for the shear effects, can be compared with (5), which neglects the shear effects. Indeed, relationship (5) suggests that Taylor's hypothesis is approximately valid if the characteristic eddy velocity $v_e$ is much smaller than the mean velocity $\overline{u}$, i.e., $v_e << \overline{u}$. For the eddies of size $\lambda_u$ from the inertial subrange the $v_e$ can be expressed as $v_e^2 \propto [k_w S_p(k_w)] \propto \varepsilon^{2/3} k_w^{-2/3} \propto \varepsilon^{2/3} \lambda_u^{2/3}$, where $\varepsilon$ is the dissipation of the turbulent energy (e.g., Monin and Yaglom (15)). For the logarithmic layer we can assume $\varepsilon \approx u_*^3 / \kappa z$ (Grinvald and Nikora (6)), which gives $v_e^2 \propto [u_*^2 / (\kappa z)^{2/3}] \lambda_u^{2/3}$, or $v_e \propto [u_* / (\kappa z)^{1/3}] \lambda_u^{1/3}$. Thus, the condition $v_e << \overline{u}$, which is a form of condition (5), can be expressed as $[u_* / (\kappa z)^{1/3}] \lambda_u^{1/3} << \overline{u}$, or as $\lambda_u << (\overline{u} / u_*)^3 \kappa z$. A comparison of $\lambda_u << (\overline{u} / u_*) \kappa z$ for shear flows, (14), with $\lambda_u << (\overline{u} / u_*)^3 \kappa z$ for homogeneous flows shows that the shear effects impose much stronger restrictions on the scales of eddies which can be considered as 'frozen' (as $(\overline{u} / u_*) \kappa z << (\overline{u} / u_*)^3 \kappa z$).

Relationships (11), (12), and (14) provide qualitative or very approximate quantitative estimates and must be supplemented by analysis of direct measurements in open-channel flows.

## METHOD

In general, two approaches are possible for an experimental study of the applicability of Taylor's hypothesis. One of them is based on transferring time series of velocity/substance fluctuations into spatial ones, calculating correlation, structure functions, or spectra for both time and spatial series, and then testing relationships (1) to (4). Such an approach was used by Pinton and Labbe (26) to test Taylor's hypothesis for the case of swirling flows. These authors defined this approach as a local version of the 'frozen' turbulence hypothesis. Another approach is based on a direct test of (1) to (4), using measurements in both the time and spatial domains (Monin and Yaglom (15)). In this study we used the second approach. Relationship (4) was used as an analytical expression of Taylor's hypothesis in our test, i.e., we used the Fourier space rather than the 'real' space. The basic relationships of this technique are:

$$S_{pi}(k_w) = S_{pi}(\omega) \frac{d\omega}{dk_w} \tag{15}$$

$$U_E = \frac{\omega}{k_w} \quad \text{or} \quad k_w = \frac{1}{U_E} \omega \tag{16}$$

where $U_E$ = eddy convection velocity which may be viewed as an analog of the phase velocity while $d\omega / dk_w$ = an analogue of the group velocity, as in wave theory. Relationship (15) connects spectra obtained from time series, $S_p(\omega)$, and from spatial data, $S_p(k_w)$. Relationship (16) may be identified as an analog of wave dispersion relation. If turbulence is 'frozen' enough, one expects that $\omega = (U_E \equiv \overline{u}) k_w$ and so $S_{pi}(k_w) = U_E S_{pi}(\omega)$, i.e., using wave theory terminology we can identify 'frozen' turbulence as 'non-dispersive' turbulence. However, in general the eddy convection velocity $U_E$ may depend on eddy scale itself, which implies non-linearity of the relationship $\omega = U_E(\omega, k_w) k_w$. Therefore, a test of Taylor's hypothesis is equivalent to the test of the relationship

$\omega = U_E(\omega, k_w)k_w$. If $U_E(\omega, k_w) \equiv \overline{u}$ the 'frozen' turbulence hypothesis is applicable; if not, a correction may be developed based on the function $k_w = f(\omega)$, or $\omega = f_1(k_w)$. This methodology can be applied using synchronous two-point measurements with distance $\delta x$ between sensors 1 and 2 (sensor 1 is upstream, sensor 2 is downstream). Then, the following useful variables may be obtained:

$$\Delta t(\omega) = \frac{\Delta\varphi(\omega)}{\omega}; \quad \text{and} \quad U_E(\omega) = \frac{\delta x}{\Delta t(\omega)} \tag{17}$$

where $\Delta\varphi(\omega)$ is the phase spectrum defined as $\Delta\varphi(\omega) = arctg\{-Q_{12}(\omega)/C_{12}(\omega)\}$; $Q_{12}(\omega)$ and $C_{12}(\omega)$ are sine (quad or imaginary) and cosine (real) parts of the cross-spectrum between points 1 and 2, respectively (Monin and Yaglom (15); Bendat and Piersol (1); Grinvald and Nikora (6)); $\Delta t(\omega)$ is the time-shift spectrum, i.e., the time interval for a spectral component of frequency $\omega$ to travel from point 1 to point 2. Using (17) we can obtain wave-numbers $k_w$ as:

$$k_w = \frac{\Delta t(\omega)}{\delta x}\omega \tag{18}$$

which now can be related to the corresponding frequencies to test the relationship $k_w = f(\omega)$. The above procedure provides a workable method for testing Taylor's hypothesis using just two-point measurements. Indeed, it is hardly possible in field conditions to measure velocities synchronously at enough spatial points to get a sufficiently detailed wave-number spectrum.

To evaluate the bulk eddy convection velocity we used the cross-correlation method:

$$U_E = \frac{\delta x}{\tau_{\max}} \tag{19}$$

where $\tau_{\max}$ = time lag in the cross-correlation function $R_{12}(\tau)$ between points 1 and 2 corresponding to the maximum ordinate of $R_{12}(\tau)$. Relationship (19) provides the same information as (17) if turbulence is 'non-dispersive'. Otherwise, estimates from (19) will be biased by the largest eddies. In our analysis we use relationship (19) for comparison purposes as most previous open-channel studies (e.g., Grinvald and Nikora (6); Nikora and Ekhnich (18); Nikora (17); Shteinman et al. (29)) were mainly based on this method.

## MEASUREMENTS

Field experiments were conducted in the Balmoral Irrigation Canal (North Canterbury, New Zealand). The experimental section was chosen 585 m downstream of the intake and about 350 m above the sediment pond. The cross-sectional shape of the channel is close to trapezoidal with top width of 6.2-7.0 m, bottom width of 3.5-4.5 m, and depth of 1 m. The bed material in the central flat part of the channel was greywacke gravel with $d_{50}$=10 mm. The measurements used in this study were conducted on 26 of February 1997. During that day the background hydraulic conditions varied insignificantly (water depth within 2%, flow rate within 4%, and slope within 7%). To minimise side-wall effects, all measurements were conducted at the central vertical. The main hydraulic parameters for the experiments were: flow rate Q = 5.14 $m^3/s$; cross-sectional mean velocity $U_a$ = 1.05 m/s; cross-sectional mean depth $H_a$ = 0.78 m; hydraulic radius $R$ = 0.70 m; depth at the measuring vertical $H$ = 1.05 m; global Reynolds number $\mathrm{Re} = U_a R/\nu$ = 0.74x10$^6$; global Froude number $Fr = U_a/\sqrt{gR}$ = 0.40; bed particle Reynolds number $\mathrm{Re}_* = u_* d_{50}/\nu$=694 (at the measuring vertical); shear velocity $u_*$ = 6.94 cm/s (obtained from the Reynolds stress measurements); and $u_*/u_{*_c} \approx 1$ where

$u_{*c} = (\tau_c / \rho)^{0.5}$, $\tau_c$ is the critical bed shear stress for particles of $d_{50}$=10 mm (at the measuring vertical). Thus, the measurements were conducted at weak bed-load transport which was close to critical (i.e., the bed shear stress was close to its critical value for given bed material). Concentration of suspended particles, 4 to 230 μm in diameter with the mean size 50-70 μm, varied from 0.003 to 0.006 g/l. Therefore, the measured suspended sediments may be fairly considered as a passive substance (Monin and Yaglom (15)).

The measurements were conducted using Acoustic Doppler Velocimeters (ADV), with the sampling volume 10 cm away from transducer (Kraus et al. (12); Lohrman et al. (13)). Experimental design included synchronous measurements of all three velocity components as well as a surrogate of suspended particle concentration (i.e., the scattered amplitude of the acoustic signal which is provided as a standard ADV routine) in two points lying on a line parallel to the mean flow with $\delta x$= 16 cm, 24 cm, 32 cm, 44 cm, and 52 cm. For each pair the flow variables were measured at 10 distances from the bed, from $z \approx 1$ cm to $z \approx 88$ cm (i.e., $0.01 \le z/H \le 0.84$). The duration of point measurements was 2 min. with a sampling interval of 0.04 s. The spatial counterpart of this temporal sampling interval (assuming that Taylor's hypothesis is applicable at this scale; this will be confirmed in RESULTS) is larger than that where attenuation due to the finite sampling volume becomes appreciable, i.e., 3 cm (Voulgaris and Trowbridge (32), p. 276). More details about the experimental set-up and equipment used may be found in Nikora and Goring (20).

The preliminary analysis of the measured data set comprised two stages. First, the data were extracted from the initial binary files and checked for unreliable records. About 15% of the initial ADV files were rejected as unreliable because of high level of Doppler noise and spikiness (Nikora and Goring (19); Voulgaris and Trowbridge (32)). The rejected ADV files had the correlation coefficient $\overline{R^2} < 67$ and signal-to-noise ratio $\overline{SNR} < 13$. Note that $\overline{R^2}$ and $\overline{SNR}$ are parameters characterising uncertainty in ADV measurements (Kraus et al. (12); Lohrman et al. (13)). The thresholds $\overline{R^2} = 67$ and $\overline{SNR} = 13$ are slightly lower than those suggested by Sontek/Nortek for individual samples, i.e., 70 and 15, respectively. We selected these lower thresholds as the calculated turbulence parameters for records with $67 \le \overline{R^2} \le 70$ and $13 \le \overline{SNR} \le 15$ showed no anomalous behaviour compared to those values obtained for $\overline{R^2} > 70$ and $\overline{SNR} > 15$. The files with $\overline{R^2} < 67$ and/or $\overline{SNR} < 13$ showed appreciable deviation from the remaining 'good' data, especially the skewness and kurtosis coefficients, and therefore were rejected. Second, to minimise errors in turbulence characteristics related to the sensor misalignment (that may cause leakage of the longitudinal velocity component into other two components), velocity records were corrected. The correction procedure (Goring et al. (5); Nikora and Goring (20)) was based on an assumption that the flow well above the bed but still far from the water surface was close to uniform two-dimensional, i.e., it satisfied the conditions $\overline{v} = 0$, $\overline{w} = 0$, and $\overline{v'w'} = 0$. This procedure was applied for 5-6 points far from the bed and the water surface in each velocity profile, and three misalignment angles were obtained for each sensor at each point. Then, assuming that the sensors kept the same orientation for all points within the profile and any differences between points were due to statistical variability, the angles were averaged and used to correct the velocities at all points within each profile. In most cases the misalignment angles in the data-set used were less than $1.8^o$.

We used the time series $S(t) = 10^{pI(t)}$ as a surrogate for suspended sediment concentration where $I(t)$ is the scattered amplitude of the acoustic signal provided by the ADV, and $p$ is a coefficient (Lohrmann et al. (13)). The correlation between mean values of $S$ and directly measured suspended sediment concentration appeared to be high enough ($r^2 = 0.95$) to consider $S$ as an appropriate surrogate for suspended sediment concentration.

The measurement noise of individual probes is not correlated and, therefore, the noise contributions to the two-point cross-correlation functions and cross-spectra, used in this study, are negligible. Thus, the inherent ADV noise does not bias the estimates of $\Delta t(\omega)$, $\tau_{\max}$, and $U_E(\omega)$. The main sources of errors in $U_E(\omega)$ relate to the errors in $\delta x$ (which is less than 1%), $\tau_{\max}$, and $\Delta t(\omega)$. The errors in $\tau_{\max}$ are less than the sampling interval, while the errors in $\Delta t(\omega)$ depend on the

sampling interval, the number of freedom degrees in the phase spectra estimates, and/or the coherence function (Bendat and Piersol (1)). The total random error in $U_E$ also depends on the distance between probes (it increases with decrease in $\delta x$), and on eddy scale (or frequency $\omega$). Our estimates show that the relative standard errors in $U_E$ were in the range from 4 to 15% in the near-bed region and from 10 to 35% in the near-surface region. All calculations for this study were done using the ADVANS package (Goring et al. (5)) specially developed by our team for various turbulence analyses of ADV data.

Details about the turbulence structure and the suspended sediment-turbulence relations for this case study may be found in Nikora and Goring (20) and in Nikora et. al. (21). Here we present graphs only for relative turbulence intensities (Fig. 1) which characterise turbulence properties important to the problem of Taylor's hypothesis applicability (see relations (5) and (6)).

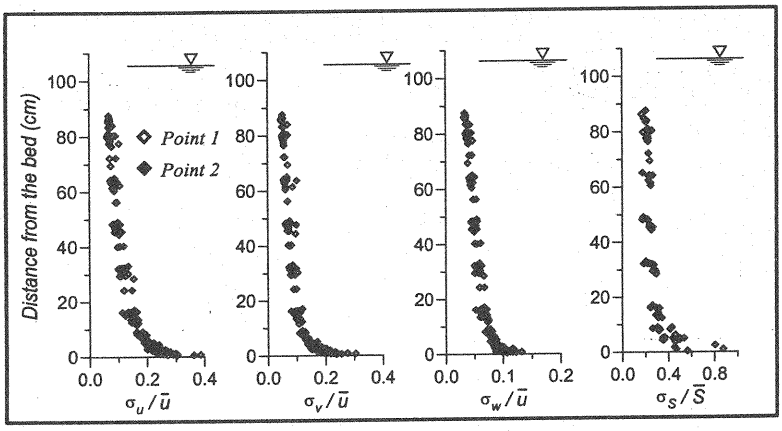


Fig. 1 Relative turbulence intensities for velocity components and passive substance, from ADV measurements in the Balmoral Canal.

## RESULTS

*Bulk eddy convection velocity*

The cross-correlation functions between corresponding velocity components at the upstream and downstream points showed properties similar to those earlier reported for the component $u$ for fixed-bed open-channel flows (e.g., Shteinman et al. (29)). They all have quasi-symmetrical shape with maxima in the negative range of time lags $\tau$, which means that the signal firstly appears at the upstream point and then, with time delay (lag) $\tau_{max}$, at the downstream point. Also, functions $R_{12}(\tau)$ for velocities (Fig. 2) clearly show that characteristic time scales (or correlation lengths) are the largest for the velocity component $u$, intermediate for the component $v$, and minimal for the vertical velocity $w$. Cross-correlation functions for $S$ appeared to be very similar to those for the vertical velocity $w$, i.e., characteristic time scales of $S$ were much smaller than those for the longitudinal and transverse components of the velocity vector. These features are evident in Fig. 2 which presents an example of functions $R_{12}(\tau)$ for $\delta x = 16$ cm. In most cases the level of maximum correlation $R_{12}(\tau_{max})$ decreased with increase in $\delta x$.

Comparisons between the bulk eddy convection velocities for $u$, $v$, $w$, and $S$, and the mean local velocity $\bar{u}$ are presented in Fig. 3. The vertical distribution of $U_E$ can be subdivided into two regions. The first one is the $\approx 10$ cm thick near-bed region where $U_E$ is larger than $\bar{u}$. The difference between $U_E$ and $\bar{u}$ in this region increases towards the bed. This feature is especially noticeable for $u$, $v$, and $S$ while the vertical velocity component $w$ shows the least deviation from $\bar{u}$. The flow region above this near-bed layer behaves differently: deviations of $U_E$ from $\bar{u}$ in this region are not systematic and are

comparable with errors involved in the determination of $U_E$ (as the estimates of $\bar{u}$ are much more accurate). The velocity gradient $\partial \bar{u} / \partial z$ corresponding to the boundary between the two regions is in the range of 1.7 to 2.3 $s^{-1}$. It increases towards the bed just as the turbulence intensity does (Fig. 2). It is worth noting that similar effects in respect to the component $u$ were also found for lowland river reaches with fixed beds (e.g., Shteinman et al. (29)).

*Dispersion relation*

Some examples of the functions $\Delta t\,(\omega)$ for all the measured variables ($u$, $v$, $w$, and $S$) are shown in Fig. 4. One can see in this figure that for near-bed measurements the eddy travel time $\Delta t\,(\omega)$ between two measuring points increases with frequency. However, for measurements well above the bed $\Delta t\,(\omega)$ is approximately constant. Another typical feature of the functions $\Delta t\,(\omega)$ is the jump at high frequencies which corresponds to switching from $2\pi$ to 0 in the phase spectra (when $\Delta\varphi\,(\omega)$ exceeds $2\pi$). We have not interpreted these high frequency regions in $\Delta\varphi\,(\omega)$ because in most cases the coherence between the two signals in these regions was close to or below the 95% confidence level (Bendat and Piersol (1)).

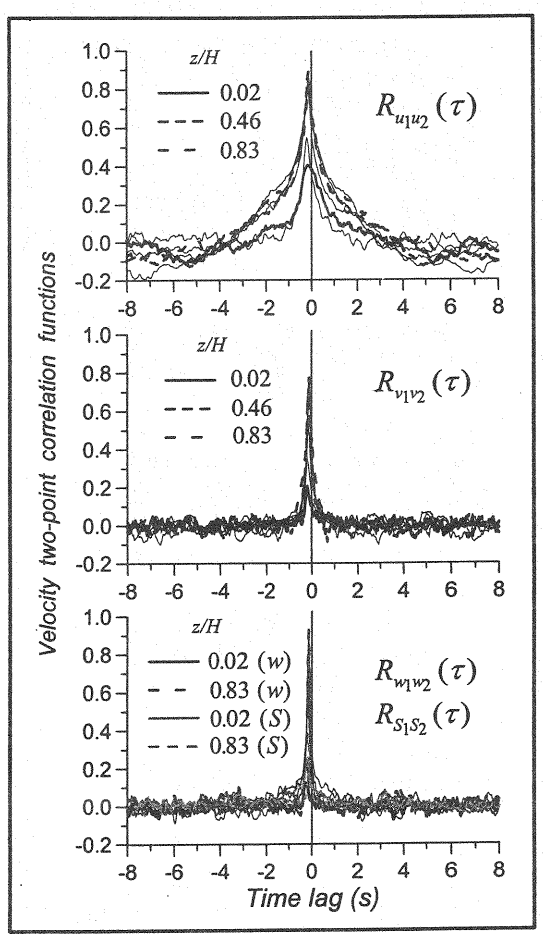


Fig. 2 Cross-correlation functions for velocity components and passive substance at two points separated by $\delta x = 16\ cm$. Thin solid lines define cross-correlation functions for the intermediate $z/H$ between 0.02 and 0.83. Note that only lines for $z/H$=0.02, 0.46, and 0.83 are highlighted, for clarity.

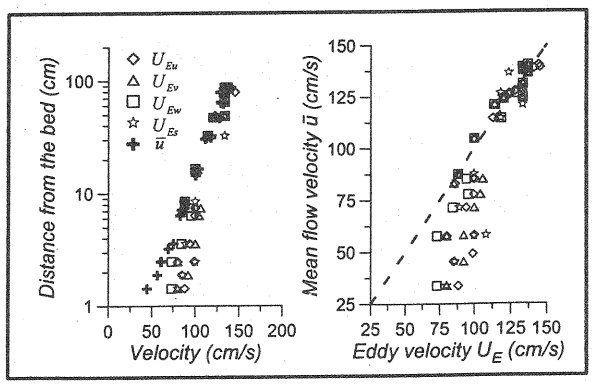


Fig. 3 Comparison between the local mean velocity $\bar{u}$ and the eddy convection velocities $U_{Eu}$ (for longitudinal velocity $u$), $U_{Ev}$ (for transverse velocity $v$), $U_{Ew}$ (for vertical velocity $w$), and $U_{ES}$ (for passive substance).

Fig. 5 shows an example of the dispersion relationship (16) obtained from the time-shift spectra from Fig. 4 using (18). The dashed lines in the graphs correspond to the relation between wave number and frequency, $k_w = \omega / \overline{u}$, which would occur if Taylor's hypothesis were valid (upper lines correspond to the near-bed measurements, while low ones to the near-surface measurements). As one can see on these graphs, the near-bed measurements clearly deviate from the predicted relation $k_w = \omega / \overline{u}_b$ where $\overline{u}_b$ is the near-bed mean velocity, i.e., $\overline{u} = \overline{u}_b$. The degree of this deviation increases with frequency decrease, or the eddy scale increase. At the lowest resolved frequencies (large eddy scales) the experimental near-bed points lie near the low dashed lines which correspond to $k_w = \omega / \overline{u}_s$ with the near-surface mean velocity $\overline{u} = \overline{u}_s$. However, at high frequencies (small eddy scales) the experimental points are fairly close to the prediction from Taylor's hypothesis, when the near-bed mean velocity is used (the upper dashed lines $k_w = \omega / \overline{u}_b$, Fig. 5). Between these two extremes the dispersion relationship for the near-bed flow region may be approximated, in most cases, as $k_w = m\omega^{\mu}$ where the exponent $\mu$ is larger than 1 and close to 1.2. The largest deviations of the near bed measurements (i.e., at $z/H$=0.02) from the power approximation $k_w \propto \omega^{\mu}$ (thick solid lines in Fig. 5) are random and do not exceed 30%. The squared correlation coefficients for this approximation were in the range from 0.973 to 0.991.

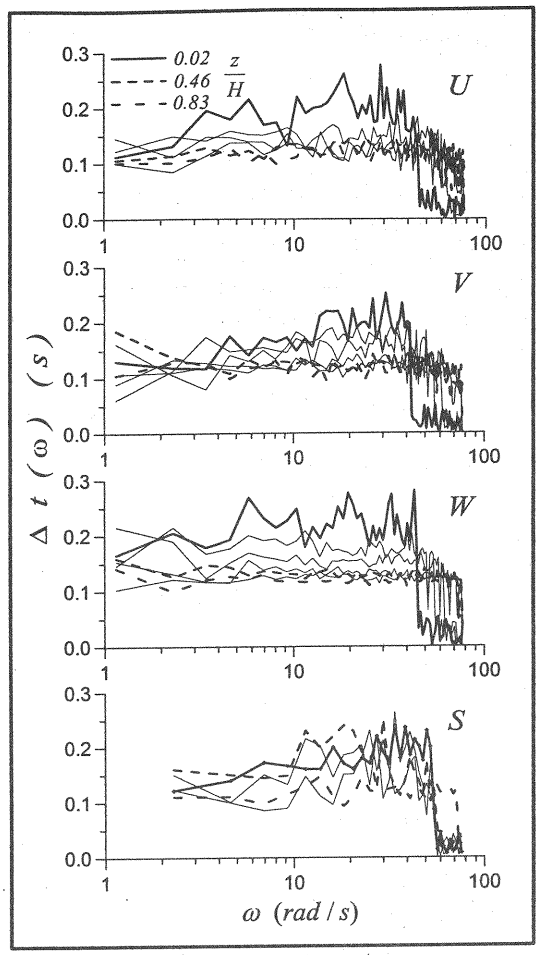


Fig. 4 Time-shift spectra for longitudinal ($u$), transverse ($v$), and vertical ($w$) velocities, and for passive scalar ($S$); $\delta x = 16\ cm$. Thin solid lines define time-shift spectra for the intermediate $z/H$ between 0.02 and 0.83. Note that only lines for $z/H$=0.02, 0.46, and 0.83 are highlighted, for clarity.

A careful examination of the dispersion graphs in Fig. 5 shows some difference between the variables which occur for the near-bed measurements. Whereas, the dispersion graphs for $u$, $v$, and $S$ are quite similar to each other, that for the vertical velocity component is slightly different, namely, it is closer to the Taylor's relation $k_w = \omega / \overline{u}_b$ than those for $u$, $v$, and $S$. The critical wave numbers defined by (11) and (12) for the near-bed region, where vertical gradients of $\overline{u}$ are significant, are also shown in Fig. 5. As one can see, they agree with direct measurements quite well indicating the wave number above which Taylor's hypothesis should apply. The above features of the dispersion relation for the near-bed region can be summarised as in Fig. 6. The range of scales where the approximation $k_w = m\omega^{\mu}$ is valid depends on the difference between the near-bed mean velocity, $\overline{u}_b$, and the propagation velocity for the largest eddies, $\overline{u}_t$ (which in our case may be approximated by the mean velocity at $z/H = 0.83$), i.e.:

$$\frac{\overline{u}_b}{\overline{u}_t} = (\frac{\omega_b}{\omega_t})^{1-\mu} \qquad (20)$$

As the distance from the bed increases, the exponent $\mu$ quickly tends to 1. In agreement with the correlation analysis, the boundary between flow regions with $\mu > 1$ and with $\mu \approx 1$ is located at approximately 10 cm from the bed. The empirical functions $k_w = f(\omega)$ for the upper flow region may be fairly well approximated by Taylor's relation $k_w = (1/\overline{u})\omega$ (Fig. 5).

A comparison between the two approaches, (17)-(18), and (19) shows that the correlation function method, (19), may help to identify the difference between $U_E$ and $\overline{u}$ but provides rather qualitative information about $U_E$. Indeed, for the near-bed region the estimates from (19) gave values for $U_E$ which corresponded to those for eddies of intermediate scales (where relation $k_w = m\omega^{\mu}$ is valid). A more complete description of $U_E$ is provided by the dispersion relation $k_w = f(\omega)$ (Figs. 4 and 5).

## DISCUSSION

### *On the applicability of Taylor's hypothesis for open-channel flows*

In our study we found that Taylor's hypothesis is applicable for the flow region away from the bed where the spatial gradients of the mean velocity $\overline{u}$ and the relative turbulence intensities $\sigma_i / \overline{u}$ are small. This agrees with previous studies in rivers and boundary layers (Monin and Yaglom (15); Grinvald and Nikora (6)) and with theoretical analyses (Ogura (22); Gifford (4); Monin and Yaglom (15)). We also showed that Taylor's hypothesis works fairly well in this flow region for a passive substance.

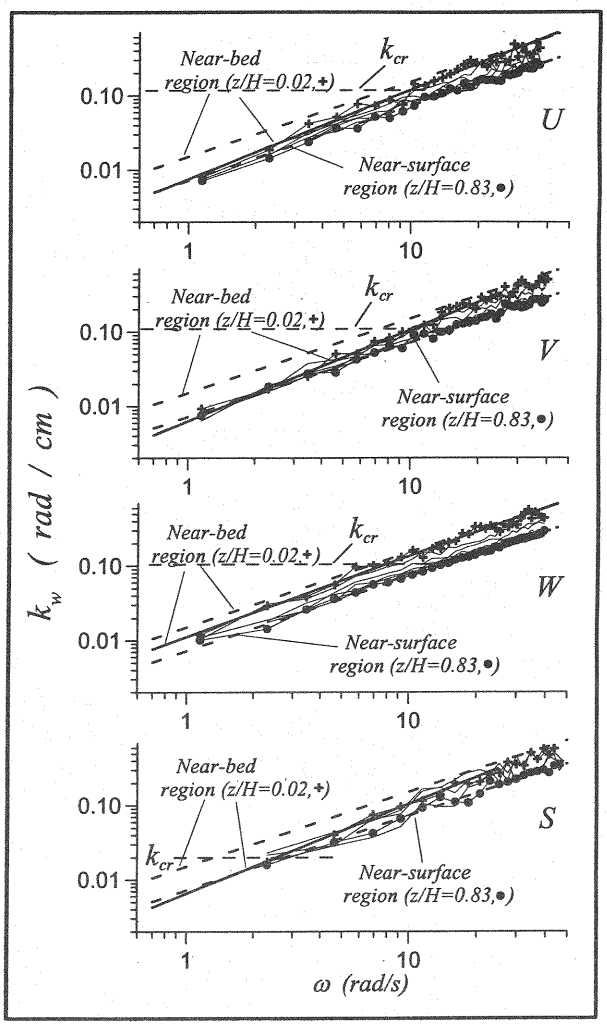


Fig. 5 Empirical dispersion relations for longitudinal ($u$), transverse ($v$), and vertical ($w$) velocities, and for passive scalar ($S$) ($\delta x = 16\ cm$). Dashed lines correspond to predictions from Taylor's hypothesis, $k_w = (1/\overline{u})\omega$, i.e., in each figure the upper dashed line is for the near-bed region while the lower dashed line is for the near-surface region. The thick solid lines show power approximations $k_w = m\omega^{\mu}$ for $z/H$ =0.02 while the thin solid lines define empirical dispersion relationships for the intermediate $z/H$, between 0.02 and 0.83. Only symbols for $z/H$=0.02 (crosses) and $z/H$=0.83 (circles) are shown, for clarity.

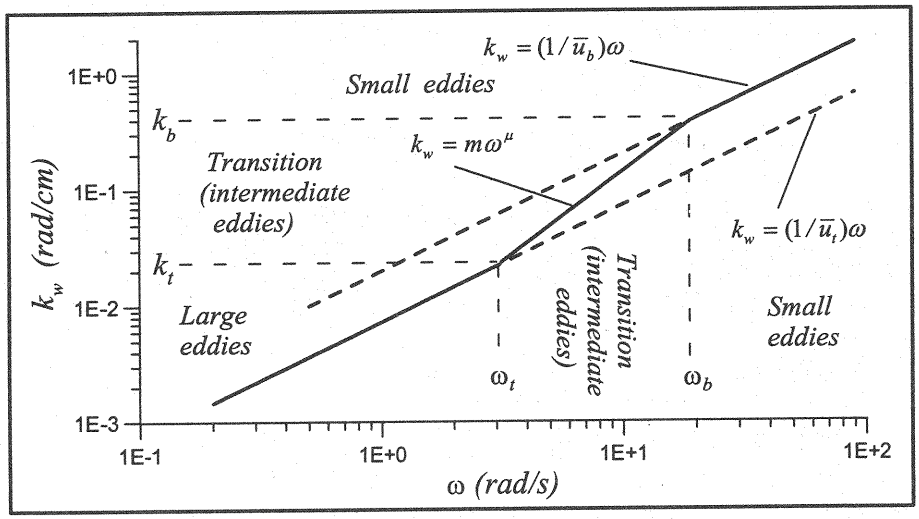


Figure 6. Sketch for the dispersion relation $k_w = f(\omega)$ in the near-bed flow region.

A simple rule of the thumb to define the flow region where Taylor's hypothesis with $U_E = \overline{u}$ may be used is $z/H > 0.10$. This estimate is based on both the present study and our previous work for lowland rivers (Grinvald and Nikora (6); Nikora and Ekhnich (18); Nikora (17); Shteinman et al. (29)). Thus, the flow can be subdivided into two regions: *(1)* a near bed region, $z/H < 0.10$, where the eddy convection velocity $U_E$ depends on the eddy scale and so Taylor's hypothesis requires a correction; and *(2)* an upper flow region, $z/H > 0.10$, where Taylor's hypothesis is applicable, and $U_E = \overline{u}$.

Fig. 5 and the sketch in Fig. 6 suggest that small-scale eddies with length-scales less than 0.15-0.25 flow depths travel downstream with a speed $U_E$ which is close or equal to the local mean velocity $\overline{u}$. This agrees well with criteria (11) and (12) which can be used for preliminary estimates. This characteristic of small scale eddies is valid for both the near-bed region with relatively high velocity gradients and turbulence intensities, and for the upper flow region with low velocity gradients and relatively low level of turbulence (Figs. 1 and 5). The same situation occurs for intermediate and large scale eddies if $z/H > 0.10$. However, in the near-bed region the travel speed of eddies with wave-numbers (or frequencies) smaller than $k_b$ (or $\omega_b$) (see Fig. 6) increases with eddy scale until $U_E(k,w)$ reaches the bulk flow velocity (in our case it was fairly close to $\overline{u}$ at $z/H = 0.83$). Then any further increase in eddy scale (larger than 3-6 flow depths) does not change the convection velocity. These features imply that Taylor's hypothesis still can be used for small ($k > k_b$) and large ($k < k_t$) eddies but with different convection velocities (see Fig. 6). In the range of intermediate scales, $k_b > k > k_t$, this hypothesis cannot be used as the eddy convection velocity changes with the scale, i.e., $k_w = m\omega^{\mu}$. In relation to spectra this problem can be resolved if a modified hypothesis is used, i.e., instead of (4) a more general relationship (15) is implied with the following dispersion relations:

$$\left.\begin{aligned} k_w &= \frac{1}{U_E}\omega \quad \text{with} \quad U_E = \overline{u} \quad \text{for} \quad k > k_b \\ k_w &= m\omega^{\mu} \quad \text{for} \quad k_b > k > k_t \\ k_w &= \frac{1}{U_E}\omega \quad \text{with} \quad U_E = \overline{u}_a \quad \text{for} \quad k < k_t \end{aligned}\right\} \qquad (21)$$

where $\overline{u}_a$ = bulk flow velocity (as a first approximation we would suggest the vertically averaged velocity as $\overline{u}_a$). To use (15) together with (21) the wave-numbers $k_b$ and $k_t$ at the limits need to be defined. Our data (e.g., Fig. 5) show that, as the first approximation, these wave-numbers may be expressed in the non-dimensional form as $k_t H \approx 1.4$ and $k_b H \approx 30$. Thus, our results suggest that for the near-bed region we should use three equations, instead of a single equation (4):

$$S_p(k_w = \omega / \overline{u}) = \overline{u} S_p(\omega) \qquad \text{for} \quad \omega \geq \omega_b \tag{22}$$

$$S_{pi}(k_w = m\omega^{\mu}) = S_{pi}(\omega)\frac{d\omega}{dk_w} = \frac{1}{m\mu}\omega^{1-\mu} S_{pi}(\omega) \qquad \text{for} \quad \omega_t \leq \omega \leq \omega_b \tag{23}$$

$$S_p(k_w = \omega / \overline{u}_a) = \overline{u}_a S_p(\omega) \qquad \text{for} \quad \omega \leq \omega_t \tag{24}$$

Equations (22) to (24) show that the shape of the frequency spectrum is preserved in the wave number spectrum at low and high wave numbers, subject to equations (22) and (24). However, in the range of the intermediate wave numbers the shape of the wave number spectrum will be different from that of the frequency spectrum, subject to equation (23). Indeed, in the range $\omega_t \leq \omega \leq \omega_b$ (Fig. 6) the spectral slope $\xi_\omega$ in the frequency domain will relate to that $\xi_k$ in the wave number domain as $\xi_\omega = \mu(\xi_k + 1) - 1$. For instance, if $\omega_t \leq \omega \leq \omega_b$ covers the inertial subrange we have $\xi_k = -5/3$ which, bearing in mind that $\mu \approx 1.2$, gives $\xi_\omega \approx -1.8$. However, for $\xi_k = -1$ we have the same slope in the frequency domain, i.e., $\xi_\omega = -1$.

*Near-bed effects*

What physical mechanisms could cause such behaviour of the dispersion relation for the near-bed region? This region is characterised by both high turbulence intensities and velocity gradients and so both features could contribute to such behaviour. Indeed, the existence of the range of scales with $k_w = m\omega^{\mu}$ supports Ogura (22) and Gifford (4) theoretical analyses for flows with high $\sigma_{ui} / U_o$. If the range $k_b > k > k_t$ covers the inertial subrange, the exponent $\mu = 1.2$ gives $\gamma = -\xi_\omega - 1 \approx 0.8 > 2/3$ in $D(\tau) \propto \tau^{\gamma}$. This also agrees with earlier Hutchings' (8) observations for the atmospheric boundary layer (Auckland data, New Zealand). Similar dependence of $U_E$ on eddy scale was also found for the near-surface atmospheric layer in Davison (2) and Kaimal (9) (see also Kaimal and Finnigan (10) for a review) who reported that large scale eddies (thermal plumes) travel with higher speed than small scale ones. Such a behaviour was explained by thermal effects rather than dynamic ones. For instance, Davison (2) suggested that a plume translation speed should be close to the mean wind speed near the top of the surface shear zone as this provides a lower thermal instability level than any other possible translation speed. Although the above observations show some qualitative agreement with our data, they cannot be used directly since our experiments were free of any density driven instabilities.

Another data-set, more suitable for comparison with our results, was obtained in a wind tunnel and in a pipe by Perry et al. (24) and Perry and Li (25) (measurements were conducted at neutral conditions). Comparing their experimental spectra for the inner flow region with theoretically developed expressions they found that the spread of empirical points in the low wave-number region was higher than could be expected. Perry et al. (24) and Perry and Li (25) explained this lack of collapse of data by the possible invalidity of Taylor's hypothesis with $U_E = \overline{u}$ for the inner region. To explain these observations they used Townsend's attached-eddy hypothesis (Townsend (31)) and its later modifications and developments (Perry and Chong (23); Perry et al. (24); Perry and Li (25)). Translating this hypothesis to the conditions of open-channel flows, we can imagine the flow as a hierarchy of eddies growing from the bed (their lower parts are 'attached' to the bed and therefore this

hypothesis is known as "the attached-eddy hypothesis"). It is natural to assume that the travel speed $U_E$ of these eddies in the near-bed region depends on their scale (or height). According to this scheme, the smallest near-bed eddies should travel with the speed which is close to the local mean velocity $\overline{u}$. At the other extreme, the largest eddies with scale (or height) of the flow depth should travel with a much higher speed than the near-bed mean velocity. Also, any further increase in eddy scale cannot change their convection velocity, which is of order of the bulk flow velocity (say, the vertically averaged velocity $\overline{u}_a$). The eddy convection velocities for intermediate scales decrease from $\overline{u}_a$ to $\overline{u}$ with the decrease in eddy scale (height). Even though this conceptual model simplifies the real situation, it does allow for the existence of three regions (21) and so explains our results fairly well. Moreover, according to the attached-eddy hypothesis, most of the energy in the vertical velocity component comes from eddies commensurable with the distance from the bed. This implies that for the vertical velocity both the correlation method (19) and the dispersion relation method (17)-(18) should show the least deviation (in comparison with *u*, *v*, and *S*) from Taylor's hypothesis predictions when $U_E = \overline{u}$ is used. Indeed, this effect was noted from both techniques (see Figs. 3 and 5).

*Potential applications in hydraulic engineering*

Taylor's 'frozen' turbulence hypothesis connects spatial/wave-number measures of turbulence with temporal/frequency measures. Thus, the main applications of this hypothesis relate to turbulence measurements and their interpretations, especially for field experiments where spatial turbulence measurements encounter great difficulties. There are many hydraulic problems whose solutions are based, implicitly or explicitly, on Taylor's 'frozen' turbulence hypothesis. These problems can be subdivided into at least four groups. The first group relates to testing and verification of hydraulic models based on turbulence closures (e.g., Rodi (28)). Indeed, predictions from such models are usually compared with point-measurements which are used to obtain the turbulent energy dissipation, mixing length, or eddy viscosity. The methods for their estimation often assume validity of Taylor's 'frozen' turbulence hypothesis (e.g., Monin and Yaglom (15)). This group also includes problems relating to experimental tests of spectral turbulence models. The second group relates to developments and tests of turbulence closures based on laboratory and field experiments. For instance, to develop an empirical or semi-empirical relationship for the mixing length from point measurements, one needs to convert temporal measurements into the spatial domain, which requires validity of Taylor's 'frozen' turbulence hypothesis. The third group combines sediment transport problems which involve sediment-turbulence interactions and development of phenomenological and predictive models for sediment transport. One such problem is that of obtaining information on the spatial extent of bursting events, regarded as an important mechanism in sediment transport, from point measurements (e.g., Drake et al. (3)). Finally, the fourth group of problems refers to measurement methods in fluvial hydraulics, which are based on the use of Taylor's 'frozen' turbulence hypothesis. An example is the inertial dissipation method for estimating bed shear stress from single-point measurements (e.g., Huntly (7); Lopez and Garcia (14)). This method is based on Kolmogorov's relationship for velocity spectra in the inertial subrange (e.g., Monin and Yaglom (15)):

$$S_{pi}(k_w) = c_i \varepsilon^{2/3} k_w^{-5/3} \tag{25}$$

where subscript $i$ refers to a velocity component $u$, $v$, or $w$, $c_i$ are Kolmogorov's constants ($c_u = 3/4c_v = 3/4c_w$), $\varepsilon$ is the turbulent energy dissipation rate, and $k_w$ is the longitudinal wave-number. The method assumes that the energy production is equal to the energy dissipation, and the turbulent shear stress is approximately constant. These assumptions, which are approximately valid in the near-bed logarithmic region, lead to the relationship $\varepsilon = u_*^3 / \kappa z$. Then, using $\varepsilon = u_*^3 / \kappa z$, and additionally assuming validity of Taylor's 'frozen' turbulence hypothesis [i.e., $\overline{u} S_p(\omega) = S_p(k_w = \omega/\overline{u})$, $U_E = \overline{u}$] one can obtain from (25):

$$u_*^2 = [\frac{S_{pi}(\omega)\omega^{5/3}}{c_i}](\frac{\kappa z}{\overline{u}})^{2/3} \qquad (26)$$

Relationship (26) is often used for estimates of the bed shear stress $\tau_o = \rho u_*^2$ from single-point velocity measurements in the near-bed region, where $\varepsilon = u_*^3 / \kappa z$ is reasonably valid. However, this may not be correct because of the lack of validity of Taylor's 'frozen' turbulence hypothesis. In our open-channel flow study we found deviations from this hypothesis for $z/H \leq 0.10$. Thus, if relationship (26) is used for estimates of the bed shear stress in this flow region, it may give systematic errors up to 20-30%. Our results suggest that relationship (26) should be used for the region $0.10 < z/H < 0.20$ only, where both Taylor's 'frozen' turbulence hypothesis and relationship $\varepsilon = u_*^3 / \kappa z$ are reasonably valid. Thus, this example shows that an incorrect assumption of the validity of Taylor's 'frozen' turbulence hypothesis may lead to significant errors in measured flow parameters.

## CONCLUSIONS

1. For the flow region $z/H > 0.1$ the eddy convection velocity is close to the local mean velocity and the Taylor hypothesis of 'frozen' turbulence is applicable to convert time-structure and time-correlation functions, and frequency spectra into space-structure and space-correlation functions, and wave-number spectra.

2. For the near-bed flow region, $z/H < 0.1$, the eddy convection velocity demonstrates dependence on eddy scale with the existence of three scale regions with different types of dispersion relations (21). These relations can be used for converting time/frequency turbulence characteristics into spatial/wave-number ones and therefore may be identified as a modified Taylor's hypothesis.

3. The attached-eddy hypothesis provides a quite plausible explanation for the anomalous behaviour of the dispersion relation for the near-bed flow region. This shows that studies of Taylor's hypothesis are important, not only for resolving the technical problem of frequency-wave-number conversion, but also for building a physically-based model of turbulence structure in open-channel flows.

4. Further studies of the Taylor hypothesis based on accurate measurements and more adequate methods are necessary. One such method is a wavelet based analysis. In comparison with our techniques of cross-correlation functions and time-shift spectra, which deal with the average behaviour over the duration of the measurement, wavelets provide the opportunity to track the trajectory of eddies of various scales with time. This feature of wavelets may help better understand the applicability of Taylor's hypothesis and give a new insight into the structure of open-channel turbulence.

## ACKNOWLEDGMENTS

The research was conducted under contracts NIW701 from the Marsden Fund administered by the Royal Society of New Zealand, and CO1818 from the Foundation for Research Science and Technology (New Zealand). The authors are grateful to D.M. Hicks, S. Brown, and M. Duncan for assistance with field measurements and data analysis. T. Komatsu, R. Ettema, and two anonymous reviewers provided helpful comments and suggestions which we gratefully incorporated into the paper.

## REFERENCES

1. Bendat, J.S. and A.G. Piersol : Engineering Applications of Correlation and Spectral Analysis, John Wiley and Sons, New York, 1980.
2. Davison, D.S. : The translation velocity of convective plumes, Quart. J. R. Met. Soc., 100, pp.572-592, 1974.

3. Drake, T.G., R.L Shreve, W.E. Dietrich, P.J. Whiting and L.B. Leopold : Bedload transport of fine gravel observed by motion-picture photography, J. Fluid Mech., 192, pp.193-217, 1988.
4. Gifford, F. : The relation between space and time correlations in the atmosphere, Journal of Meteorology, 13, pp.289-294, 1956.
5. Goring, D.G., V.I. Nikora and S.L.R. Brown : ADVANS: A suite for turbulence analysis of ADV data. Manual. Part 1, NIWA Internal Report No 11, pp.1-55, 1998.
6. Grinvald, D.I. and V.I. Nikora : River Turbulence (in Russian), Hydrometeoizdat, Leningrad, Russia, 1988.
7. Huntley, D.A. : A modified inertial dissipation method for estimating seabed stresses at low Reynolds numbers, with application to wave/current boundary layer measurements, J. of Phys. Oceanogr., 18, pp.339-346, 1988.
8. Hutchings, J.W. : Turbulent theory applied to large-scale atmospheric phenomena, Journal of Meteorology, 12, pp.263-271, 1955.
9. Kaimal, J.C. : Translation speed of convective plumes in the atmospheric surface layer, Quart. J. R. Met. Soc., 100, pp.46-52, 1974.
10. Kaimal, J.C. and J.J. Finnigan : Atmospheric Boundary Layer Flows, Oxford University Press, Oxford, 1994.
11. Khinchin, A. Ya. : Korrelationstheorie der stationaren stochastischen prozesse, Math. Ann., 109(4), pp.604-615, 1934.
12. Kraus, N.C., A. Lohrmann and R. Cabrera : New acoustic meter for measuring 3D laboratory flows, J. of Hydr. Engrg, ASCE, 120(3), pp.406-412, 1994.
13. Lohrmann, A., R. Cabrera and N.C. Kraus : Acoustic Doppler velocimeter (ADV) for laboratory use, Proc., Symp. on Fundamentals and Advancements in Hydr. Measurements and Experimentation, edited by C.A. Pugh, ASCE, New York, NY, pp.351-365, 1994.
14. Lopez, F. and M. Garcia : Wall similarity in turbulent open-channel flow, J. of Engrg. Mech., ASCE, 125(7), pp.789-796, 1999.
15. Monin, A.S. and A.M. Yaglom : Statistical Fluid Mechanics: Mechanics of Turbulence, vol. 2, MIT Press, Boston, Mass., 1975.
16. Nezu, I., and H. Nakagawa : Turbulence in Open-Channel Flows, A.A. Balkema, Rotterdam, Brookfield, Netherlands, 1993.
17. Nikora, V. : Channel Processes and Hydraulics of Small Rivers (in Russian), Shtiintsa, Kishinev, Moldova, former USSR, 1992.
18. Nikora, V. and M. Ekhnich : On applicability of the frozen turbulence hypothesis in river flows (in Russian), Meteorology and Hydrology (Russia), 3, pp.98-103, 1991.
19. Nikora, V.I. and D.G. Goring : ADV turbulence measurements: can we improve their interpretation?, J. of Hydr. Engrg., ASCE, 124(6), pp.630-634, 1998.
20. Nikora, V.I. and D.G. Goring : Effects of bed mobility on turbulence structure, NIWA Internal Report No 48, Christchurch, pp.1-48, 1999.
21. Nikora, V.I., D.G. Goring and D.M. Hicks : Suspended-sediment and turbulence interactions in a gravel-bed flow with weak bed-load, J. of Hydr. Res., IAHR (submitted).
22. Ogura, Y. : The relation between the space- and time-correlation functions in a turbulent flow, J. Meteor. Soc. Jap., 31, pp.355-369, 1953.
23. Perry, A.E. and M.S. Chong : On the mechanism of wall turbulence, J. Fluid Mech., 119, pp.173-217, 1982.
24. Perry, A.E., S. Henbest and M.S. Chong : A theoretical and experimental study of wall turbulence, J. Fluid Mech., 165, pp.163-199, 1986.
25. Perry, A.E. and J.D. Li : Experimental support for the attached-eddy hypothesis in zero-pressure-gradient turbulent boundary layers, J. Fluid Mech., 218, pp.405-438, 1990.
26. Pinton, J-F. and R. Labbe : Correction to Taylor's hypothesis in swirling flows, Advances in Turbulence 5, Proc. of the 5$^{th}$ European Turbulence Conference, Kluwer Academic Publishers, pp.418-421, 1995.

27. Piomelli, U., J-L. Balint and J.M. Wallace : On the validity of Taylor's hypothesis for wall-bounded flows, Phys. of Fluids A, 1(3), pp.609-611, 1989.
28. Rodi, W. : Turbulence Models and Their Applications in Hydraulics, A.A. Balkema, Rotterdam, Brookfield, Netherlands, 1993.
29. Shteinman, B., V. Nikora, M. Ekhnich and A. Sukhodolov : An experimental validation of the "frozen" turbulence hypothesis for river flows, Advances in Turbulence 6, Proc. of the 6th European Turbulence Conference, Kluwer Academic Publishers, pp.531-532, 1996.
30. Taylor, G. : The spectrum of turbulence, Proc. Roy. Soc., A164 (919), pp.476-490, 1938.
31. Townsend, A.A. : The Structure of Turbulent Shear Flows, Cambridge University Press, Cambridge, 1976.
32. Voulgaris, G. and J.H. Trowbridge : Evaluation of the Acoustic Doppler Velocimeter (ADV) for turbulence measurements, Journal of Atmospheric and Oceanic Technology, 15, pp.272-289, 1998.
33. Zaman, K.B.M.Q. and A.K.M.F. Hussain : Taylor hypothesis and large-scale coherent structures, J. Fluid Mech., 112, pp.379-396, 1981.

## APPENDIX - NOTATION

The following symbols are used in this paper:

| | |
|---|---|
| $D(\tau)$ | = temporal velocity/substance structure function; |
| $D(\Delta x)$ | = spatial velocity/substance structure function; |
| $H$ | = flow depth; |
| $k_w$ | = wave-number; |
| $R(\tau)$ | = temporal velocity/substance auto-correlation function; |
| $R(\Delta x)$ | = spatial velocity/substance auto-correlation function; |
| $R_{12}(\tau)$ | = temporal velocity/substance cross-correlation function between points 1 and 2; |
| $S$ | = instantaneous passive substance concentration; |
| $\overline{S}$ | = mean passive substance concentration; |
| $S_{\max}$ | = maximum passive substance concentration; |
| $S_p(\omega)$ | = frequency auto-spectrum of the *i*-th velocity component or substance; |
| $S_p(k_w)$ | = wave-number auto-spectrum of the *i*-th velocity component or substance; |
| $U_E$ | = eddy convection velocity; |
| $U_{max}$ | = maximum (surface) velocity; |
| $u$ | = instantaneous longitudinal component of velocity vector; |
| $\overline{u}$ | = local mean (longitudinal) velocity; |
| $u_*$ | = shear velocity; |
| $v$ | = instantaneous transverse component of velocity vector; |
| $w$ | = instantaneous vertical component of velocity vector; |
| $z$ | = distance from the bed; |
| $\delta x$ | = distance between sensors; |
| $\sigma_{ui} = (\overline{u_i'^2})^{0.5}$ | = standard deviation of *i-th* velocity component; |
| $\sigma_S = (\overline{S'^2})^{0.5}$ | = standard deviation of passive substance concentration; |
| $\tau$ | = time lag; |
| $\tau_{max}$ | = time lag corresponding to the maximum ordinate of $R_{12}(\tau)$; |
| $\omega$ | = frequency; |
| $\Delta t(\omega)$ | = time-shift spectra; and |
| $\Delta x$ | = spatial lag. |

(Received April 14, 2000 ; revised September 4, 2000)